Research Paper

Journal of Engineering and Technological Sciences

Design Optimization of Automobile Wheel Rim by Using Taguchi-SAW Method

Ngoc Thai Huynh[1], Anh Son Tran[2], Anh Cuong Ho[2], Van Nang Do[2,*], Minh Hung Vu[3], & Quoc Manh Nguyen[4]

[1]Faculty of Mechanical Engineering and Technology, Ho Chi Minh City University of Industry and Trade, 140 Le Trong Tan, Tay Thanh Ward, Ho Chi Minh City 700000, Vietnam
[2]Faculty of Automotive Engineering and Technology, Industrial University of Ho Chi Minh City, 12 Nguyen Van Bao street, Hanh Thong Ward, Ho Chi Minh City, 700000, Vietnam
[3]Faculty of Fundamental Sciences, PetroVietnam University, Ho Chi Minh City 700000, Vietnam
[4]Faculty of Mechanical Engineering, Hung Yen University of Technology and Education, Hung Yen 160000, Vietnam

*Corresponding author: dovannang@iuh.com.vn

Abstract

In the automotive industry, reducing vehicle weight while maintaining durability is crucial for improving fuel efficiency, reducing emissions, and enhancing overall vehicle performance. The wheel rim is a vital component that supports the vehicle's load and influences unsprung mass, directly affecting ride quality and safety. Therefore, designing an optimized wheel rim that minimizes weight without compromising strength under heavy load conditions is essential. This research investigates three materials—aluminum alloy, magnesium alloy, and titanium alloy—known for their high strength-to-weight ratios and suitability for automotive applications. Three key geometric design variables were considered: spoke thickness (t), spoke width (w), and spoke radius (r), each tested at three different levels. Finite Element Analysis (FEA) was conducted using ANSYS software to evaluate stress distribution and deformation of various design configurations under typical operational loads. Optimization was performed using the Simple Additive Weighting (SAW) multi-criteria decision-making method to identify the most effective design balancing multiple objectives. To ensure the reliability of results, statistical methods including the Taguchi method, analysis of variance (ANOVA), interaction analysis, and regression analysis were applied for validation. The optimized wheel rim design achieved an 11% weight reduction compared to the baseline model, with maximum stress and deformation values of 29.106 MPa and 0.0459 mm, respectively. These closely matched the predicted values, showing errors of only 0.66% and 0.31%, confirming the accuracy of the model. This study demonstrates a successful approach to producing a lightweight, durable wheel rim that can contribute to improved vehicle efficiency and reduced manufacturing costs.

Keywords: *finite element analysis; MEREC method; SAW method; structural wheel rim; Taguchi method.*

Introduction

The need to travel is an essential for everyone. Therefore, manufacturing vehicles to run on the roads is very necessary. Vehicles require a very high level of safety for both passengers and car itself. As a result, careful calculation is required in the design and manufacture of vehicle parts. While the vehicle is in motion, the rim bears a significant load. Consequently, careful selection of materials is necessary to ensure both durability and lightweight design. This reduces fuel consumption and manufacturing costs. This is a big challenge for researchers. The wheel rim was designed by CATIA software (Ashok et al., 2021). The design modeling was tested in three cases by UG/NX NASTRAN. The test results in 3 cases proved that the stress of the wheel rim is less than the yield stress of the material. An optimized rim structure achieved a weight reduction of 4.08%. The selection of materials for the wheel rims is specifically analyzed using ANSYS software (Abhiman et al., 2021). A modal analysis and a dynamic analysis were also performed to test the performance of the wheel rim. Carbon fiber and magnesium alloy (Zhang et al., 2025) were used to manufacture the wheel rim. The dimensions of the optimal wheel rim model were obtained through simulation and experiments. The weight of the suggested model was reduced by 13.08%. To achieve a 27% weight reduction, an innovative design of the aircraft wheel rim made of carbon fiber-reinforced plastic was proposed (Wacker et al., 2021). The tests and finite element analysis (FEA) results show that the structure of the aircraft wheel rim meets the requirements for use. The weight of the electric wheel is reduced by up to 58% due to the use of composite materials (Joglekar et al., 2021). The analytical results show

ISSN: 2337-5779
DOI: 10.5614/j.eng.technol.sci.2026.58.4.9

DOI: 10.5614/j.eng.technol.sci.2026.58.4.9

that the proposed model meets the working requirements. The results of the radial fatigue test, cornering fatigue test, and FEA (Vinchu & Chaudhari, 2021) revealed that the wheel rim, made from two different materials, meets the safety criteria specified by IS and ARAI standards. To reduce weight and meet the requirements of the wheel rim, three different materials are used (Sharma et al., 2021). The results of the FEA and experiments show that the wheel rim made from magnesium alloy material exhibits lower stress than the other two materials. Static and dynamic analyses for the automobile wheel rim structure (Gadwala & Babu G, 2022) were performed using ANSYS workbench. The wheel rim structure is designed using CATIA software. The FEA of the wheel rims made from two different materials was performed (Karim & Ku, 2022). The results revealed that the wheel rims made from 6061 aluminum alloy exhibited lower stress and strain displacements compared to those made from magnesium alloy. There are numerous surveys on the methods of manufacturing the wheel rims and the materials used in their production (Gebrehiwet et al., 2022). The survey results show that the wheel rims made from aluminum alloy are the most popular with spokes, steel discs, or light alloys. The processes used to manufacture the wheel rims include casting and forging. The stress and deformation distributions of 20 the wheel rim models were determined using the finite element method (Özdemir et al., 2022). A genetic algorithm was used to select the wheel rim model with low stress and strain distribution, and the aesthetic model was selected as the optimal model. The Wheel rims require very careful testing of their performance and are costly and time-consuming. Therefore, to reduce the cost and time, FEA was used (Parihar & Chakraborty, 2022) to measure the deformation and stress of the wheel rims made from different materials while the vehicle was moving at 100 km/h. The results indicated that the wheel rims made from magnesium alloy were the most durable because they had the lowest stress distribution. An angular fatigue analysis was conducted to reduce weight when designing an aluminum alloy wheel rim using FEA in ANSYS (Shinde et al., 2022). The analysis results revealed that the stress of the wheel rim is smaller than the yield stress of the aluminum alloy. FEA was conducted on the wheel rims made of 7079 aluminium alloy reinforced with 8% carbon fiber (CF) (Somayaji et al., 2022). The vibration frequency of 7079 aluminum alloy the wheel rims reinforced with carbon fiber was higher than that of the wheel rims made of other materials. The honeycomb wheel rim (Wang et al., 2022) achieves load-bearing performance, resulting in a 12.61% reduction in the total weight of the wheel rim. The stiffness, hardness, and durability meet the design requirements. All these results are achieved thanks to the results of FEA. Different types of forces acting on the wheel rims made from different materials were analyzed using FEA (Patil & Chavan, 2023). The experiment on the wheel rim under bending load was conducted to confirm the results of the FEA. The Wheel rims made from aluminum alloy are less expensive than those made from magnesium alloy (Loganathan & Subramani, 2023). The FEA results demonstrated that the wheel rims made from aluminium alloy are 58.3% lighter than those made from magnesium alloy, while still meeting safety standards. In order to achieve a reasonable spoke wheel rim structure with low deformation and stress, FEA was performed (Majumder et al., 2023). The Simulation outcomes of this wheel rim with different materials have been specifically analyzed. The performance of spoked the wheel rims made from different materials, such as aluminum alloy, magnesium alloy, and titanium alloy, is compared based on finite element analysis results in ANSYS (Padmanabhan et al., 2023).

The comparison results indicated that the spoke wheel made from magnesium alloy is the best, with less stress and deformation than the wheel rim made from the other two materials. The weight of the spoked wheel rim is optimized to be reduced by 4.49% by using the modified NSGA-II optimization algorithm and weighted grey relational analysis (Zhang et al., 2023) based on the results of the wheel rim bending and radial fatigue analysis using the finite element method. Experiments are also conducted to validate the results of the proposed methods. The fatigue of a 25-inch industrial rim (Danzi et al., 2024) was analyzed in earth-moving machines by Moveero, following a design change reducing thickness from 11 mm to 9 mm. The critical area identified was the seat radius of the fixed flange, highly stressed due to tire bending. Laboratory tests in the U.S. examined various load and pressure conditions, with strain data used to model tire-rim contact pressure. FEM simulations in SolidWorks then assessed stress distribution and predicted fatigue life under different loading scenarios. The structural integrity of the 2024–2025 UAH Moonbuggy Team's ATHENA rover wheels (Dawson, 2025) was analyzed . Designed for improved strength and reduced weight, the wheels and hubs underwent FEA to assess performance under high loads. Made from 6061-T6 aluminum and 1018 steel, the components achieved a safety factor of 1.4, confirming reliability for NASA's HERC course. During competition, a hard landing caused suspension damage, but the wheels remained intact, helping the team complete the second run and secure 3rd place. The design and analysis the car wheel rims made from different materials—AM60B magnesium alloy and two aluminium alloys (Al-7068, AlSi7Mg0.3) were performed using ANSYS 2025 R1 (Kumar & Chandrashekhar, 2025). Under identical loading conditions, simulations assessed deformation and stress levels. Results showed that the rim made from AlSi7Mg0.3 performed best, with minimal deformation and stress, making it the most suitable for strength, durability, and efficiency. The findings support using AlSi7Mg0.3 for optimizing the wheel rim design in automotive applications. The performance of Formula 1 the wheel rim materials—Mg AZ80, Al 6061-T6, and carbon fibre—under high heat, pressure, and speed (Kepekci et al., 2025) was analyzed using CFD simulations. Results showed that carbon fibre had the lowest deformation and best thermal resistance, while Mg AZ80 deformed the most and retained more heat. Overall, carbon fibre was found to be the most suitable material for F1 wheel rims due to its superior mechanical and thermal properties. The Extended Finite Element Method (XFEM) (Montassir et al., 2024) was applied to investigate crack growth in automotive rims. By identifying critical zones and estimating fatigue life, the research accurately predicts where cracks may form. Results closely match experimental data, providing valuable insights into the structural integrity and durability of rims under repeated loading. The development of lightweight and durable wheel designs for road bicycles (Padmanabhan et al., 2023) was conducted by comparing magnesium alloys, titanium alloys and structural steels. Two modern spoke designs were analyzed for stress and strain. Titanium showed the lowest stress concentration, while magnesium showed significantly higher deflection up to 77% higher than steel. The results support the creation of the optimal alloy wheel, balancing strength, weight and safety. SolidWorks and ANSYS were used to design and optimize the weight of the wheel rim by analyzing stress, displacement, and fatigue life under various loads (Khatiwada et al., 2025). The project compared steel, aluminum, magnesium alloy, and forged steel. The results showed that the steel alloy provided the best balance between strength, weight, and cost, making it ideal for modern wheel rims. The optimization also helped improve fuel efficiency without compromising structural integrity. Three 22-inch alloy wheel designs made from 6061-T6 aluminum were compared using FEA in SolidWorks 2019 (Alfarisi et al., 2024) for deformation and stress. Each model was tested under 3000N force and 800N pressure. Among the three models, Model 3 showed the best performance with low stress (11.02MPa), minimal displacement (0.021mm), high safety factor and safe deformation, making it the most reliable design. The safety and fatigue behavior of automotive wheels under different loading conditions was analyzed using CAD, CAE, and FEM tools (Santos et al., 2025).

Model analysis showed that the natural frequencies were in the range of 350–610 Hz. Simulations under vertical, lateral, and radial loads showed safety factors of 2.60, 2.66, and 1.76, respectively, identifying critical stress and deformation zones. These findings help improve the design efficiency, safety, and durability of wheels while reducing prototyping costs. The rolling forming of DP590 steel rims after butt welding (Song et al., 2024)was carried out using Abaqus. The software analyzed the stress, strain and thickness changes, emphasizing softening in the subcritical temperature affected zones. Friction effects were also considered, emphasizing the need to use DP590 carefully in welded wheel rims. The vibration behavior analysis of a 17-inch aluminium alloy wheel using finite element simulation in ANSYS (Wijaya et al., 2024) was performed. By adjusting the spoke angle (5°, 10°, 15°), the impact on the natural frequency and maximum deformation was evaluated. The results showed that the natural frequency was in the range of 723.2 Hz and the deformation was in the range of 22.5 mm. A composite rim made via Resin Transfer Moulding (RTM) (Zanchini et al., 2023) showed reduced weight and increased stiffness compared to aluminium alloys. Fatigue tests and FEA confirmed the safety and compliance of the composite rim, despite minor defects. The study also reviews Ferrari's rim designs since 2009, comparing materials, manufacturing methods, and performance. A shape optimization method (Zhang et al., 2025) was applied for automotive rims using a simplified 2D model and the 90° impact test. The approach improves development efficiency over traditional 3D simulations. Results show a 0.51 mm decrease in deformation and a 59 g weight reduction, enhancing both strength and lightweighting.

While numerous studies have explored the wheel rim design using aluminum alloys and conventional optimization techniques, there has been limited investigation into the performance of alternative materials such as magnesium and titanium alloys in similar loading environments. Furthermore, existing research often focuses on single-objective optimization, without considering a comprehensive framework that integrates material selection, geometric design variables, and multi-criteria decision-making.

The novelty of this study is as follows:

1. Combining material optimization and geometric design in a comprehensive model: The study simultaneously considers three lightweight materials with high strength-to-weight ratios (aluminum alloys, magnesium alloys, and titanium alloys) along with three important geometric design variables (spoke thickness, spoke width, and spoke radius). This combined evaluation in a comprehensive analytical framework represented a novel approach compared to studies that focus on only one factor.
2. Application of the SAW method in multi-criteria optimization of automotive rim design and materials: The use of the Simple Additive Weighting (SAW) method to select the optimal design configuration is a highlight, which is rare in rim design optimization studies. This method allows us to balance multiple objectives such as weight reduction, strength maintenance, and deformation control - which are often difficult to achieve with only one criterion.
3. Integrating multiple statistical analysis methods to ensure model reliability: The study uses a combination of statistical tools such as the Taguchi method, ANOVA, interaction analysis and linear regression to verify the accuracy and reliability of the simulation model. This is a systematic approach, which helps increase the practical value of the results.
4. Reducing the weight of the wheel rim by up to 11% while ensuring mechanical strength: The results show that the optimal design can reduce the weight by up to 11% while maintaining the maximum stress and deformation within

DOI: 10.5614/j.eng.technol.sci.2026.58.4.9

the safe limit, with very low errors compared to the predicted model (<1%). This demonstrates the practical effectiveness of the optimization model.

5. In this investigation, the Taguchi–SAW–MEREC method has served as a novel hybrid method that combines empirical optimization with objective multi-criteria decision making.
6. The Taguchi method is used to design the experiment and identify key parameters, providing reliable input data. Then, the MEREC method is used to determine the weights of the evaluation criteria more objectively based on their influence when omitted. These weights are then used in the SAW method to synthesize and rank the alternatives, thereby determining the optimal conditions.
7. While previous studies often combine such as Taguchi–Entropy–SAW or Taguchi–TOPSIS, the Taguchi–SAW–MEREC model offers two outstanding advantages. MEREC determines the weights objectively without relying on expert judgment, while SAW simplifies the calculation and interpretation compared to complex models such as TOPSIS or VIKOR.

In summary, this combination integrates the strengths of each component: Taguchi's strength is experimental design, while MEREC and SAW's strength is objective weighting and result aggregation for decision making, respectively. Therefore, the proposed model has the advantage of being simple and efficient for multi-criteria optimization in engineering applications, representing a novel contribution beyond the traditional Taguchi-based approaches.

Design of Automobile Wheel Rim

The wheel rim model in this investigation was designed using Inventor software. The frame size and diameter wheel rim follow Honda's standards. Based on the CR-V SUV model shown in Figure 1, the wheel rim has 7 spokes. The spoke thickness, spoke width, and spoke diameter were selected as design variables.

Figure 1 The automobile wheel rim model.

Finite Analysis Model

We designed 27 models and set up the deformation and stress analysis of the model using the finite element method in ANSYS which is set up as follows:

Aluminum alloy, magnesium alloy, and titanium alloy, which have position ratios of 0.33, 0.35, and 0.36, respectively as recorded in Table 1, were selected to set up the FEA in this investigation. The model was meshed by automatic method with an element size of 2 mm. The meshing result obtained 1062829 quadrilateral elements and 1831238 nodes, as presented in Figure 2.

The fix support tool was used to fix the wheel rim thanks to the center hole, as seen in Figure 3. Applying gravity acceleration to the model is the next step to ensure that it will produce the most accurate outcome. Lastly, the force of 3240 N impacted the wheel rim.

Figure 2 Finite element model.

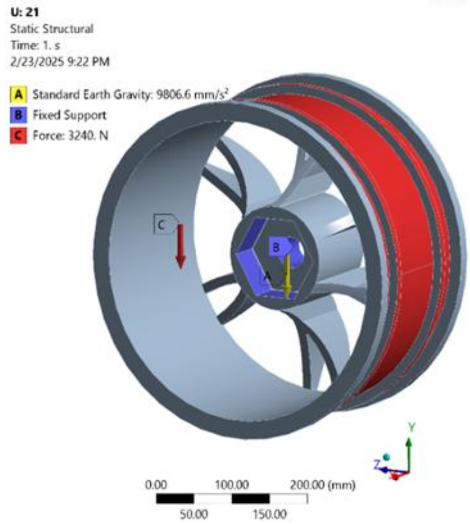

Figure 3 Loaded wheel rim model and boundary conditions.

Table 1 Mechanical properties

Material	Young's Modulus, E (GPa)	Yield Strength, σy (MPa)	Density, ρ (kg/m³)	Poisson's Ratio, ν
Aluminum Alloy	70	150	2700	0.33
Magnesium Alloy	45	100	1800	0.33
Titanium Alloy	110	900	4500	0.36

SAW Method

In this investigation, the confirmation of the optimal values of the displacement and the stress was performed by the SAW method (Ciardiello & Genovese, 2023; Jazaudhi'fi et al., 2024; Tafazzoli et al., 2024; Taherdoost, 2023) as following:

Step 1: Determine the normalized values of every criterion

$$n_{ij} = \frac{y_{ij}}{\max y_{ij}} \quad (1)$$

$$n_{ij} = \frac{\min y_{ij}}{y_{ij}} \quad (2)$$

Step 2 :

$$V_i = \sum_{j=1}^{n} w_j . n_{ij} \quad (3)$$

Where w_j is the weight of each objective, which is determined by the MEREC method

Step 3: Determine the rank of the V_i The optimal case is the case where the value of V_i is the largest.

Determine The Weight

The weight of each objective, which is determined by the MEREC method (Borchers & Pieler, 2010; Fan et al., 2024; Keshavarz-Ghorabaee, 2021; Keshavarz-Ghorabaee et al., 2021; Shanmugasundar et al., 2022) as following:

Determine performance for each case

$$S_i = \ln\left[1 + \left(\frac{1}{n}\sum_j^n \left|\ln(h_{ij})\right|\right)\right] \quad (4)$$

Determine effective performance after removing single criteria

$$S'_{ij} = ln\left[1 + \left(\frac{1}{n}\sum_{k,k\neq j}^{n} \left|ln(h_{ij})\right|\right)\right] \quad (5)$$

Determine the deviation of the criteria

DOI: 10.5614/j.eng.technol.sci.2026.58.4.9

$$E_j = |S'_{ij} - S_i| \quad (6)$$

Determine the weight for each objective

$$w_j = \frac{E_j}{\sum_k^m E_k} \quad (7)$$

Taguchi Method

To confirm the influence of design variables on the deformation and stress of the proposed model, which was obtained by FEA in ANSYS and the reliability of the SAW method. In this investigation, the Taguchi method (Barragán-Trinidad et al., 2023; Hisam et al., 2024; Jakupi et al., 2024; Kruzel et al., 2023) was utilized. Because the deformation and stress requirements of the model must be minimal to meet the working requirements, the weight of the model must be reduced to ensure a lightweight structure and lower cost. Therefore, the target of deformation and stress as small as possible was implemented as follows:

$$S/N = -10\log\left(\frac{1}{n}\sum_{i=1}^{n}\frac{1}{y_i^2}\right) \quad (8)$$

$$CI_{CE} = \pm\sqrt{F_\alpha(1, fe)Ve\left(\frac{1}{n_{eff}} + \frac{1}{R_e}\right)} \quad (9)$$

$F_\alpha(1, fe)$ obtained by **Table B-2** (Roy, 2010).

Taguchi–SAW–MEREC sequence: Identify factors → Design experiments → Collect data Standardization → Apply MEREC to determine weights → Apply SAW to select the optimal case → Calculate S/N ratio → Confirm the optimal case and the influence of design variables on the deformation and stress of the rim. Interaction analysis confirms the influence of design variables. ANOVA results significance: Identify important factors, contribution ratio, test statistical significance → guide to optimize factors. Plot analysis confirms the influence of design variables on the deformation and stress of the wheel rim as presented in Figure 4 as flow chart.

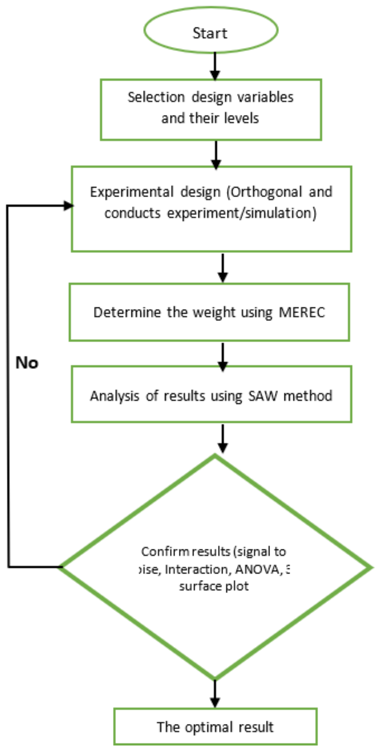

Figure 4 Flow chart of Taguchi–SAW–MEREC approach

Results

Select design variables for the wheel rim model

The Poisson ratios of the three investigated materials, namely aluminum alloy, magnesium alloy, and titanium alloy, were 0.30, 0.33, and 0.36, respectively denoted by p. The spoke thickness, denoted by t, was examined at three levels: 0.8, 0.9, and 1.0 mm. The spoke width, denoted by w, was also investigated at three levels: 1.1, 1.3, and 1.5 mm. In addition, the spoke radius, denoted by r, was assigned three levels of 16, 17, and 18 mm. The design variables and their corresponding levels are presented in Table 2.

Table 3 presents the orthogonal array and the finite element analysis results for the 27 experimental cases. A total of 27 deformation values and 27 stress values were obtained. Variations in deformation and stress were observed among the investigated cases.

The weighting results determined using the MEREC method are summarized in Table 4. The ranking and optimal alternative obtained using the SAW method are presented in Table 5. Table 6 presents the signal-to-noise ratio analysis results of the Vi values, while the analysis of variance results were summarized in Table 7.

Figure 5 illustrates the signal-to-noise ratio plots of the Vi values. Figure 6 shows the interaction plots of the average signal-to-noise ratios for the design variables. The residual plots are presented in Figure 7. Figure 8 presents the three-dimensional relationships between the Vi values and the design variables. The optimal deformation and stress distributions of the car wheel rim are shown in Figure 9.

Table 2 Designed variables and their levels

Designed variables	Symbol	Unit	Level 1	Level 2	Level 3
Poisson ratio	p		0.30	0.33	0.36
Thickness of spokes	t	mm	0.8	0.9	1.0
Width of spokes	w	mm	1.1	1.3	1.5
Spokes radius	r	mm	16	17	18

Table 3 27 simulated cases and results

Order	p	t (mm)	w (mm)	r (mm)	Deformation (mm)	Stress (MPa)
1	0.33	0.8	1.1	16	0.1192	50.6145
2	0.33	0.8	1.3	17	0.0815	39.0169
3	0.33	0.8	1.5	18	0.0610	28.6413
4	0.33	0.9	1.1	17	0.0952	58.1466
5	0.33	0.9	1.3	18	0.0680	32.8812
6	0.33	0.9	1.5	16	0.0818	36.6526
7	0.33	1.0	1.1	18	0.0793	41.3053
8	0.33	1.0	1.3	16	0.0917	44.8037
9	0.33	1.0	1.5	17	0.0657	42.1728
10	0.35	0.8	1.1	16	0.1867	59.9016
11	0.35	0.8	1.3	17	0.1276	40.8444
12	0.35	0.8	1.5	18	0.0956	34.5179
13	0.35	0.9	1.1	17	0.1490	48.6437
14	0.35	0.9	1.3	18	0.1064	37.0394
15	0.35	0.9	1.5	16	0.1279	46.4599
16	0.35	1.0	1.1	18	0.1241	41.0274
17	0.35	1.0	1.3	16	0.1434	47.1651
18	0.35	1.0	1.5	17	0.1028	43.0679
19	0.36	0.8	1.1	16	0.0896	56.3949
20	0.36	0.8	1.3	17	0.0612	31.3201
21	0.36	0.8	1.5	18	0.0459	29.1060
22	0.36	0.9	1.1	17	0.0716	49.6363
23	0.36	0.9	1.3	18	0.0511	30.6441
24	0.36	0.9	1.5	16	0.0615	38.3389
25	0.36	1.0	1.1	18	0.0598	42.2682
26	0.36	1.0	1.3	16	0.0691	45.6628
27	0.36	1.0	1.5	17	0.0495	35.6439

Table 4 MEREC method results

DOI: 10.5614/j.eng.technol.sci.2026.58.4.9

Experiment No.	h_{ij}		S_i	S'_{ij}		E_j	
	D_i	S_t		D_i	S_t	D_i	S_t
1	0.6386	0.8450	0.2688	0.2023	0.0809	0.0665	0.1214
2	0.4364	0.6513	0.4879	0.3468	0.1942	0.1411	0.1526
3	0.3269	0.4781	0.6565	0.4441	0.3140	0.2124	0.1300
4	0.5098	0.9707	0.3014	0.2903	0.0148	0.0111	0.2756
5	0.3640	0.5489	0.5907	0.4090	0.2623	0.1817	0.1467
6	0.4380	0.6119	0.5059	0.3456	0.2196	0.1603	0.1260
7	0.4251	0.6896	0.4785	0.3561	0.1705	0.1224	0.1856
8	0.4912	0.7480	0.4059	0.3041	0.1356	0.1018	0.1685
9	0.3521	0.7040	0.5290	0.4199	0.1617	0.1091	0.2583
10	1.0000	1.0000	0.0000	0.0000	0.0000	0.0000	0.0000
11	0.6836	0.6819	0.3233	0.1741	0.1752	0.1492	0.0011
12	0.5121	0.5762	0.4763	0.2886	0.2434	0.1877	0.0452
13	0.7979	0.8121	0.1963	0.1069	0.0990	0.0894	0.0079
14	0.5699	0.6183	0.4197	0.2478	0.2154	0.1719	0.0324
15	0.6854	0.7756	0.2746	0.1730	0.1196	0.1015	0.0534
16	0.6649	0.6849	0.3317	0.1857	0.1733	0.1460	0.0124
17	0.7682	0.7874	0.2243	0.1239	0.1129	0.1004	0.0110
18	0.5508	0.7190	0.3806	0.2610	0.1527	0.1196	0.1083
19	0.4799	0.9415	0.3345	0.3127	0.0297	0.0218	0.2830
20	0.3281	0.5229	0.6321	0.4429	0.2808	0.1891	0.1621
21	0.2458	0.4859	0.7239	0.5316	0.3081	0.1923	0.2234
22	0.3836	0.8286	0.4530	0.3914	0.0898	0.0616	0.3016
23	0.2740	0.5116	0.6844	0.4992	0.2890	0.1852	0.2101
24	0.3295	0.6400	0.5756	0.4416	0.2014	0.1341	0.2401
25	0.3202	0.7056	0.5560	0.4507	0.1607	0.1053	0.2900
26	0.3700	0.7623	0.4904	0.4036	0.1273	0.0868	0.2763
27	0.2653	0.5950	0.6539	0.5089	0.2308	0.1450	0.2782

Table 5 SAW method results

Experiment No.	n_{ij}		V_i	Rank
	D_i	S_t		
1	0.38487	0.56587	0.48526	24
2	0.56320	0.73407	0.65797	12
3	0.75188	1.00000	0.88949	3
4	0.48212	0.49257	0.48792	23
5	0.67523	0.87105	0.78384	6
6	0.56125	0.78143	0.68336	10
7	0.57827	0.69340	0.64213	14
8	0.50036	0.63926	0.57740	17
9	0.69800	0.67914	0.68754	9
10	0.24580	0.47814	0.37466	27
11	0.35958	0.70123	0.54907	20
12	0.47994	0.82975	0.67395	11
13	0.30804	0.58880	0.46375	26
14	0.43134	0.77327	0.62098	15
15	0.35864	0.61647	0.50164	22
16	0.36969	0.69810	0.55183	19
17	0.31999	0.60726	0.47931	25
18	0.44626	0.66503	0.56759	18
19	0.51221	0.50787	0.50980	21
20	0.74924	0.91447	0.84088	5
21	1.00000	0.98403	0.99115	1
22	0.64075	0.57702	0.60541	16
23	0.89717	0.93464	0.91795	2
24	0.74602	0.74706	0.74659	7
25	0.76754	0.67761	0.71766	8
26	0.66440	0.62723	0.64379	13
27	0.92659	0.80354	0.85834	4

Table 6 Signal to Noise Ratios of V_i

Level	p	t	w	r
1	-3.829	-3.948	-5.535	-5.276
2	-5.604	-4.011	-3.592	-4.124
3	-2.568	-4.042	-2.873	-2.601
Delta	3.037	0.094	2.662	2.674
Rank	1	4	3	2

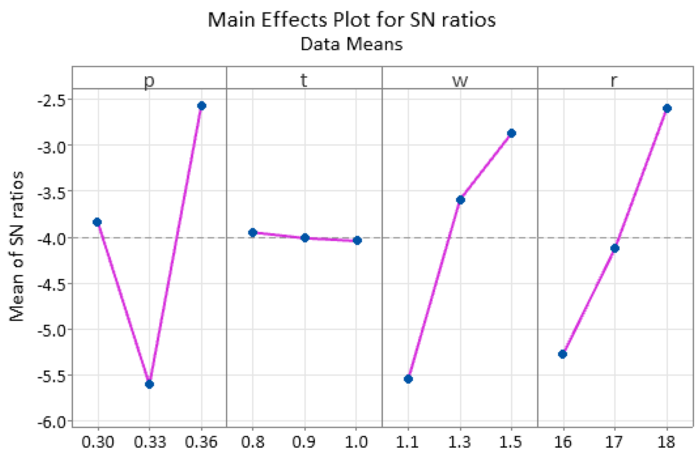

Figure 5 The graph signal to noise of V_i .

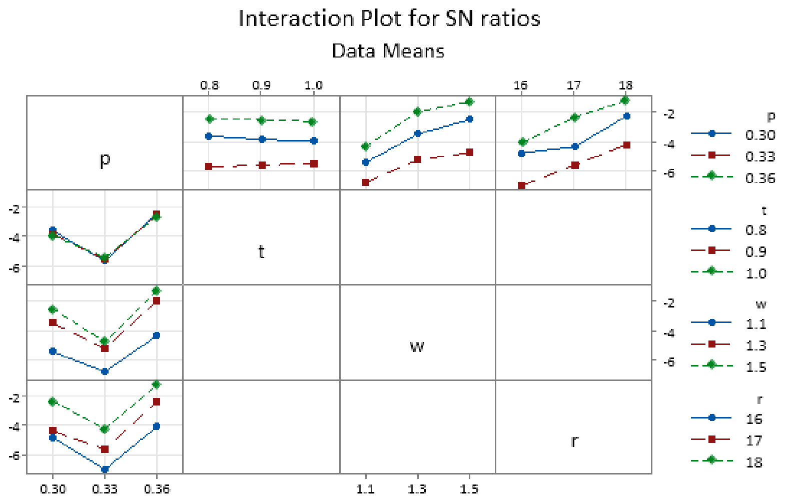

Figure 6 The graph interaction analysis of V_i signal to noise.

Table 7 Analysis of variance results of V_i

Source	DF	Seq SS	Contribution	Adj SS	Adj MS	F-Value	P-Value
p	2	0.233766	37.12%	0.233766	0.116883	369.45	0.000
t	2	0.003483	0.55%	0.003483	0.001742	5.51	0.024
w	2	0.181518	28.82%	0.181518	0.090759	286.87	0.000
r	2	0.179763	28.54%	0.179763	0.089881	284.10	0.000
p*w	4	0.016538	2.63%	0.016538	0.004135	13.07	0.001
p*r	4	0.011597	1.84%	0.011597	0.002899	9.16	0.002
Error	10	0.003164	0.50%	0.003164	0.000316		
Total	26	0.629828	100.00%				

DOI: 10.5614/j.eng.technol.sci.2026.58.4.9

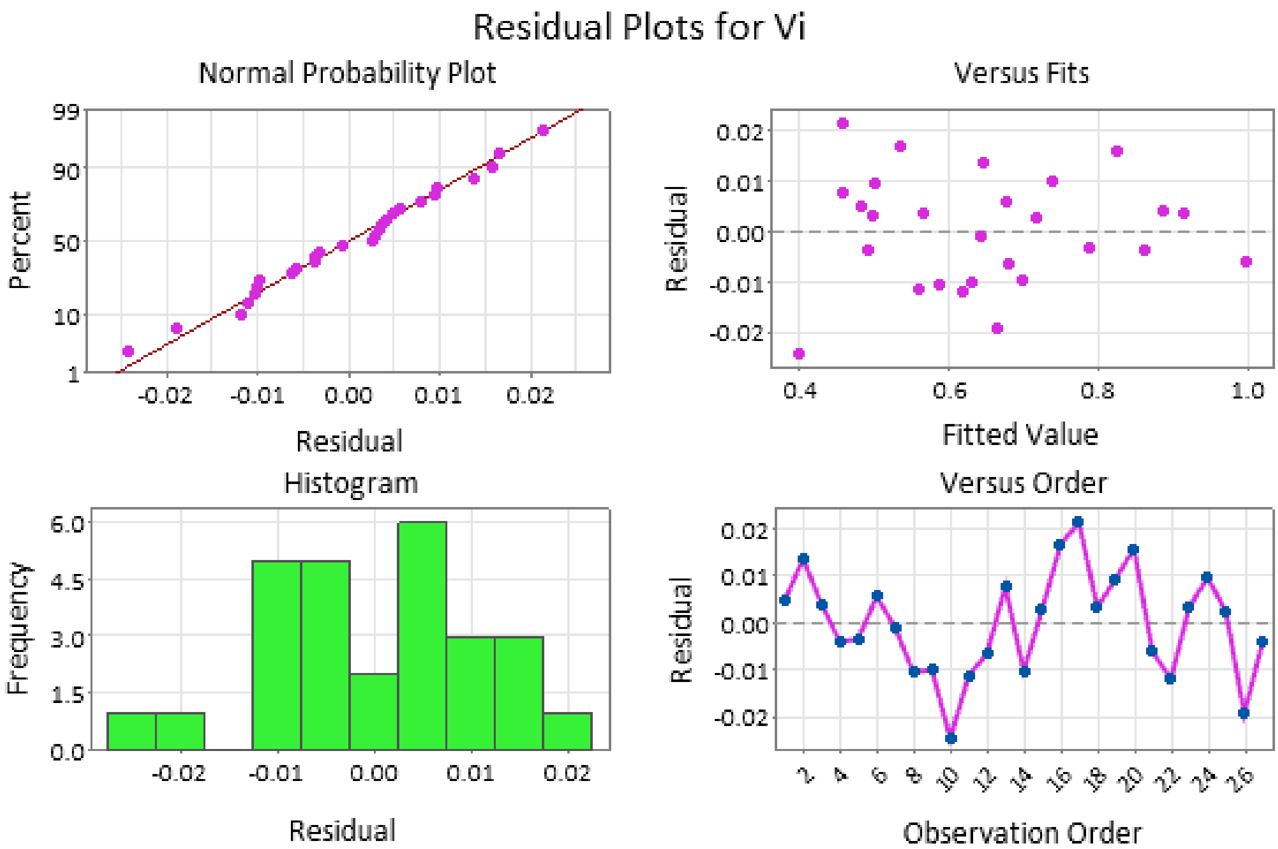

Figure 7 The graph of residual of V_i .

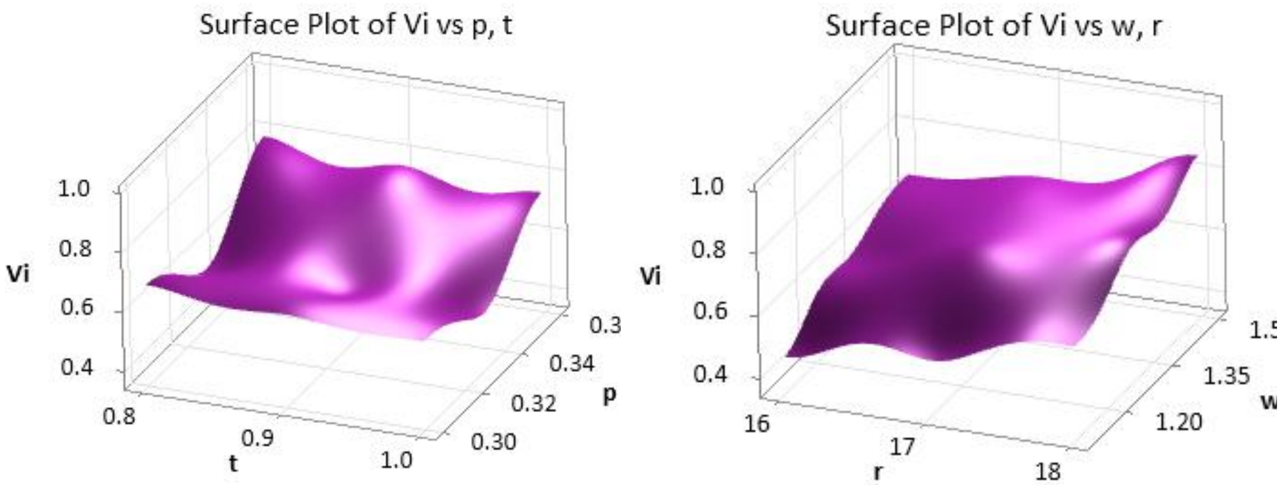

(a) Vi vs p and t

(b) Vi vs w and r

Figure 8 The graph 3D of Vi vs design variables.

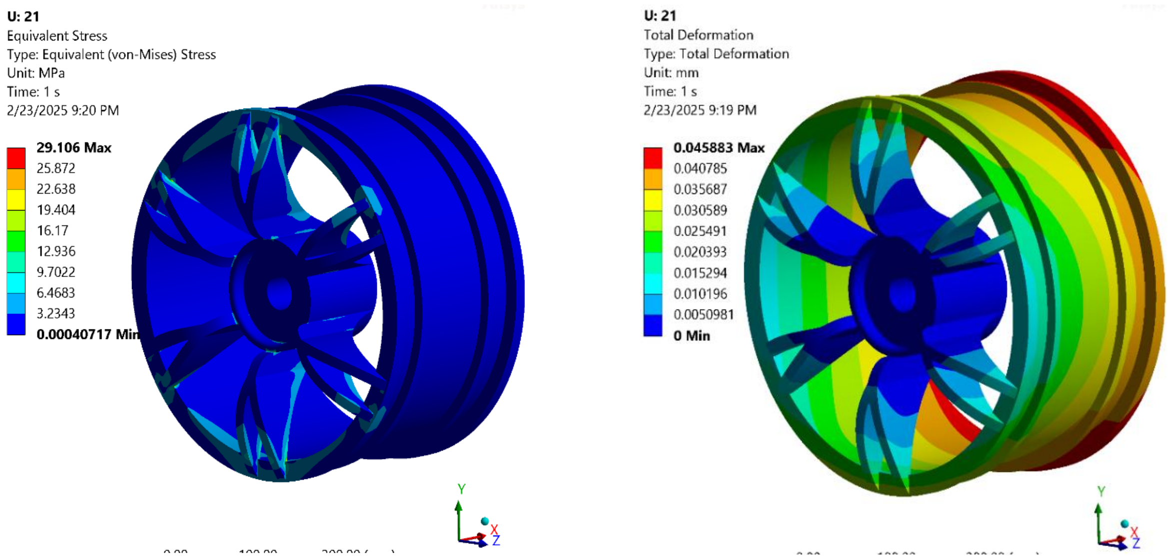

(a) Stress (b) Deformation

Figure 9 The optimum results.

Discussion

Weight determination results

The MEREC method indicated that equivalent stress had a slightly greater influence on the overall performance evaluation than deformation, with weighting factors of 0.5547 and 0.4453, respectively. This result suggests that stress distribution plays a more critical role in the structural reliability of the wheel rim under loading conditions. Since excessive stress concentration may lead to material failure and fatigue damage, assigning a higher weight to stress is mechanically reasonable for wheel rim optimization.

The obtained weighting factors also demonstrate that both deformation and stress should be considered simultaneously during the optimization process. Focusing only on deformation reduction may increase structural stiffness but could result in unfavorable stress concentration, whereas minimizing stress alone may not guarantee sufficient dimensional stability. Therefore, the combined evaluation approach provides a more balanced assessment of wheel rim performance.

SAW optimization analysis

The SAW method identified Case 21st as the optimal design configuration with the highest Vi value of 0.9915. The optimal parameter combination consisted of p=0.36, t=0.8 mm, w=1.5 mm, and r=18 mm. Among the investigated materials, the titanium alloy provided the best structural performance while reducing wheel rim weight by approximately 11%.

The superior performance of the titanium alloy can be attributed to its favorable strength-to-weight ratio and high resistance to deformation under loading conditions. In addition, increasing the spoke width and spoke radius improved load transfer capability and reduced localized stress concentration. Interestingly, the optimal spoke thickness corresponded to the minimum investigated level. This result indicates that increasing thickness alone does not necessarily improve the overall optimization objective when weight reduction is simultaneously considered.

These findings demonstrate that geometric optimization can significantly improve wheel rim performance while maintaining lightweight characteristics. Similar trends have also been reported in previous finite element studies of lightweight automotive wheel structures, where optimized spoke geometry contributed to improved structural stiffness and stress distribution.

Signal-to-noise ratio analysis

The signal-to-noise ratio analysis revealed that the Poisson ratio (p) had the greatest influence on the Vi values, followed by the spoke radius (r), spoke width (www), and spoke thickness (t). The steep slopes observed in Figure 5 indicate that variations in these parameters substantially affected the optimization response.

DOI: 10.5614/j.eng.technol.sci.2026.58.4.9

The dominant effect of the material-related parameter (p) highlights the importance of material selection in wheel rim design. Material properties directly influence stress transfer behavior and deformation resistance during loading. Meanwhile, the geometric variables (r) and www also exhibited strong effects because they control the load distribution path across the spoke structure. In contrast, the relatively smaller influence of thickness suggests that moderate thickness variations may not significantly alter the global structural response compared with material selection and spoke geometry.

The interaction plots shown in Figure 6 further indicate that interactions among design variables affected the optimization results. The non-parallel behavior of the interaction lines suggests that the influence of one parameter depended on the level of another parameter. This behavior reflects the coupled mechanical response of material properties and spoke geometry in the wheel rim structure.

Analysis of variance

The ANOVA results confirmed that the investigated variables significantly influenced the optimization response because the corresponding P-values were lower than 0.05. Among all parameters, the Poisson ratio contributed the most to the variation of the response, followed by spoke width and spoke radius. The spoke thickness exhibited the lowest contribution.

The high percentage contribution of the material-related parameter demonstrates that material selection is a dominant factor in determining the mechanical behavior of the wheel rim. This observation is consistent with the signal-to-noise ratio analysis and indicates strong agreement among the applied statistical approaches.

In addition, the high values of R square, adjusted R square, and predicted R square demonstrate that the developed regression model can accurately represent the relationship between the design variables and the optimization response. The low error contribution further indicates that the selected design factors adequately captured the primary sources of variation within the investigated design space.

Reliability and residual analysis

The residual analysis demonstrated that the developed model provided reliable and statistically acceptable predictions. As shown in Figure 7, the residual points were distributed closely around the reference line and remained approximately symmetric around zero. This behavior indicates that the residuals followed an approximately normal distribution and that no significant systematic error was observed.

Moreover, the residual values were distributed within a narrow range of approximately −0.02 to 0.02, indicating a relatively low prediction error. The absence of abnormal residual patterns suggests that the regression model was appropriate for representing the relationship between the design variables and the optimization response.

Overall, the residual analysis confirms the reliability of the finite element simulation data and supports the validity of the proposed optimization approach for wheel rim design.

$$\mathrm{V_i} = 110.3 - 662.2\mathrm{p} - 0.137\mathrm{t} + 3.03\mathrm{w} + 0.09929\mathrm{r} + 964\mathrm{p}^2 - 0.978\mathrm{w}^2 \quad (10)$$

The regression equations obtained using the Taguchi method, as presented in Eq. (10), indicate that the V_i values were strongly influenced by the investigated design variables. This relationship confirms that both material properties and spoke geometric parameters played important roles in determining the overall wheel rim performance.

The response surface plots shown in Figure 8 further illustrate the interaction between the design variables and the optimization response. As shown in Figure 8(a), the V_i values increased with increasing Poisson ratio (p) and decreased with increasing spoke thickness (t). This trend suggests that material selection had a stronger influence on the optimization response than thickness variation within the investigated range.

Figure 8(b) demonstrates that the V_i values increased as the spoke radius (r) and spoke width (w) increased. The improvement in the optimization response may be associated with enhanced load distribution and reduced stress concentration resulting from larger spoke dimensions. These observations are consistent with the finite element analysis and statistical analysis results discussed previously.

The Taguchi prediction analysis yielded an optimal V_i value of 0.9999, as presented in Table 9. The high predicted value indicates that the proposed optimization approach was effective in identifying a favorable combination of material and geometric parameters for wheel rim design. The confidence interval of the predicted V_i value was determined using Eq. (9). $CI_{CE} = \pm 0.0642,\ 0.9281 < \mu_{confirmation} < 1.0565$. Where, α = 0.05, fe = 10, F0.05(1,10) = 4.9646 (Roy, 2010), Ve = 0.000316, R =16, Re = 1, n = 27.

The optimal wheel rim configuration is presented in Figure 9. The optimized design produced relatively low equivalent stress and deformation values of 29.106 MPa and 0.045883 mm, respectively, indicating favorable structural performance under the applied loading conditions. In addition, the optimized wheel rim mass was reduced from 25.953 kg to 23.098 kg, corresponding to an approximate weight reduction of 11%.

The reduction in mass while maintaining low stress and deformation levels demonstrates the effectiveness of the proposed optimization approach in achieving lightweight structural design without significantly compromising mechanical performance. This result is particularly important in automotive applications, where weight reduction contributes to improved fuel efficiency, reduced energy consumption, and enhanced vehicle performance.

The comparison between the Taguchi prediction results and finite element analysis results further confirmed the reliability of the developed optimization model (see Table 8). The differences between the predicted and simulated values of Vi, deformation, and stress were all below 3%, indicating strong agreement between the statistical prediction model and numerical simulation results. The optimal and predicted Vi values were 0.9911 and 0.9923, respectively, corresponding to a small deviation of approximately 0.12%.

Similarly, the predicted stress and deformation values were very close to the finite element analysis results, with errors of only 0.66% and 0.31%, respectively. The low prediction errors indicate that the Taguchi-based regression model can effectively estimate the structural response of the wheel rim within the investigated design range.

Among the investigated cases, Case 21st provided the most favorable overall performance. The optimal configuration consisted of titanium alloy material with a spoke thickness of 0.8 mm, spoke width of 1.5 mm, and spoke radius of 18 mm. The superior performance of this configuration may be attributed to the high strength-to-weight ratio of titanium alloy combined with the improved load distribution provided by the larger spoke geometry.

Overall, the proposed optimization approach demonstrates strong potential for application in lightweight automotive wheel rim design. The obtained results suggest that integrating finite element analysis with Taguchi, MEREC, and SAW methods can effectively support design optimization while reducing development time and prototype iterations in automotive engineering applications.

The comparison between the present study and previously published investigations is summarized in Table 9. In general, the optimized wheel rim developed in the current study achieved relatively low stress and deformation values while simultaneously maintaining a reduced structural mass.

Compared with the study conducted by Kepekci et al., the present optimized titanium alloy wheel rim exhibited lower deformation than the magnesium alloy model and comparable performance relative to the aluminum alloy configuration. Although the carbon fiber model reported lower deformation values, composite materials generally involve different manufacturing methods, material behavior, and cost considerations compared with metallic wheel rims. Therefore, direct comparison should be interpreted carefully.

In comparison with the results reported by Padmanabhan et al. (2023), the current optimized model demonstrated substantially lower deformation and stress values for both Model A and Model B configurations. The improved performance may be associated with the combined optimization of material selection and spoke geometric parameters adopted in the present study. In particular, the integration of the Taguchi, MEREC, and SAW methods enabled simultaneous consideration of stress, deformation, and lightweight requirements during the optimization process.

Table 8 Comparison of predicted values and FEA results

Order	V_i			D_i			S_t		
	FEA results	Predicted values	Error (%)	FEA results	Predicted values	Error (%)	FEA results	Predicted values	Error (%)
1	0.4853	0.4880	0.57	0.1192	0.1175	1.45	50.6145	51.2666	1.27

DOI: 10.5614/j.eng.technol.sci.2026.58.4.9

2	0.6580	0.6518	0.95	0.0815	0.0832	2.08	39.0169	39.6070	1.49
3	0.8895	0.8929	0.38	0.0610	0.0627	2.66	28.6413	29.3591	2.44
4	0.4879	0.4913	0.69	0.0952	0.0957	0.49	58.1466	58.8644	1.22
5	0.7838	0.7866	0.35	0.0680	0.0663	2.56	32.8812	32.5734	0.95
6	0.6834	0.6772	0.91	0.0818	0.0835	2.08	36.6526	37.2427	1.58
7	0.6421	0.6360	0.97	0.0793	0.0810	2.14	41.3053	41.8954	1.41
8	0.5774	0.5808	0.58	0.0917	0.0927	1.04	44.8037	45.5215	1.58
9	0.6875	0.6903	0.40	0.0657	0.0640	2.66	42.1728	41.8650	0.74
10	0.3747	0.3850	2.69	0.1867	0.1840	1.46	59.9016	60.5283	1.04
11	0.5491	0.5463	0.50	0.1276	0.1303	2.11	40.8444	41.3635	1.26
12	0.6740	0.6664	1.14	0.0956	0.0965	0.98	34.5179	35.3720	2.41
13	0.4638	0.4562	1.66	0.1490	0.1494	0.30	48.6437	49.4978	1.73
14	0.6210	0.6313	1.64	0.1064	0.1037	2.59	37.0394	37.6661	1.66
15	0.5016	0.4989	0.55	0.1279	0.1306	2.10	46.4599	46.9790	1.11
16	0.5518	0.5491	0.50	0.1241	0.1268	2.16	41.0274	41.5465	1.25
17	0.4793	0.4717	1.61	0.1434	0.1444	0.72	47.1651	48.0192	1.78
18	0.5676	0.5779	1.79	0.1028	0.1001	2.69	43.0679	43.6946	1.43
19	0.5098	0.5068	0.59	0.0896	0.0883	1.42	56.3949	55.3912	1.81
20	0.8409	0.8316	1.12	0.0612	0.0625	2.10	31.3201	31.9016	1.82
21	0.9911	0.9999	0.13	0.0459	0.0458	0.12	29.106	29.2821	0.60
22	0.6054	0.6177	1.99	0.0716	0.0734	2.51	49.6363	49.0585	1.18
23	0.9180	0.9398	2.33	0.0511	0.0498	2.52	30.6441	31.4038	2.42
24	0.7466	0.7373	1.26	0.0615	0.0628	2.09	38.3389	38.9204	1.49
25	0.7177	0.7083	1.31	0.0598	0.0611	2.15	42.2682	42.8497	1.36
26	0.6438	0.6561	1.87	0.0691	0.0694	0.50	45.6628	46.0850	0.92
27	0.8583	0.8754	1.95	0.0495	0.0482	2.60	35.6439	36.6402	2.72

Table 9 Compare investigation results with published works

Works	Deformation (mm)	Mass(kg)	Stress (MPa)
Current investigation results	0.046 (Titanium alloy)	23.098	29.106 (Titanium alloy)
Reference (Kepekci et al., 2025)	0.097 (Al 6061-T6) 0.022 (carbon fibre) 0.14983 (Mg AZ80)		
Reference (Padmanabhan et al., 2023)	Model A 0.97445 (structural steel) 4.3271 (Magnesium alloy) 2.2075 (Titanium alloy) Model B 0.57679 (structural steel) 2.5666 (Magnesium alloy) 1.2031 (Titanium alloy		Model A 294.19 (structural steel) 293.47 (Magnesium alloy) 293.34 (Titanium alloy) Model B 142.98 (structural steel) 145.93 (Magnesium alloy) 146.63 (Titanium alloy
Reference (Khatiwada et al., 2025)	0.014 (Steel Alloy) 0.0479 (Aluminum Alloy) 0.07729 (Magnesium Alloy) 0.016547 (Forged Steel)	36.51 13.107 8.4257 35.575	47.855 (Steel Alloy) 48.163 (Aluminum Alloy) 47.57 (Magnesium Alloy) 47.662 (Forged Steel)

The present results also compare favorably with the investigation reported by Khatiwada et al (2025). Although some alloy configurations in the published work achieved slightly lower deformation values, the current model produced lower equivalent stress while maintaining a relatively lightweight structure. This finding suggests that the proposed optimization strategy can effectively balance structural stiffness and stress distribution in wheel rim design.

It should be noted that differences among the reported results are expected because each study employed different wheel geometries, material properties, loading conditions, boundary conditions, and optimization objectives. Variations in spoke configuration, rim dimensions, and applied loads can significantly influence stress transfer behavior and deformation characteristics. Therefore, direct numerical comparison between studies should be interpreted within the context of the specific modeling assumptions and design conditions adopted in each investigation.

Overall, the comparison with published studies demonstrates that the proposed optimization framework provides competitive mechanical performance while achieving meaningful weight reduction. These findings support the applicability of the proposed methodology for lightweight and structurally reliable automotive wheel rim design.

Conclusion

In this study, several design variables were selected and analyzed through finite element simulation. The materials used were aluminum alloy, magnesium alloy, and titanium alloy, with Poisson's ratios of 0.33, 0.35, and 0.36, respectively. Three geometric parameters were considered:

1. Spoke thickness (t): 0.85 mm, 0.9 mm, and 1.0 mm
2. Spoke width (w): 1.1 mm, 1.3 mm, and 1.5 mm
3. Spoke radius (r): 16 mm, 17 mm, and 18 mm

The total deformation and equivalent stress were obtained using finite element analysis (FEA). The MEREC method was employed to determine the weights of the evaluation criteria. The Simulation outcomes indicated that the selected design variables significantly influenced both stress and deformation of the wheel rim, as evidenced by the distinct outputs across all 27 simulation cases.

The consistency between the FEA outcomes and the SAW method results—reflected in the Vi values—demonstrated a strong correlation, confirming the validity of the optimization approach. Additionally, signal-to-noise ratio analysis, interaction analysis, variance analysis, regression analysis, and surface plot evaluations all supported the reliability of these findings.

The optimal Vi value was 0.9911, while the predicted Vi was 0.9923, showing a minimal deviation of only 0.12%. The optimal stress and deformation values were 29,106 MPa and 0.0459 mm, respectively, compared to predicted values of 29,282.1 MPa and 0.0460 mm. The corresponding error rates were 0.66% for stress and 0.31% for deformation, indicating high prediction accuracy and model reliability.

Although the results obtained were very reliable, the finite element analysis results have not been confirmed by experimental results. These results have not been compared with other optimization methods, such as the grey relational analysis method, TOPSIS method, WASPAS method, etc., and the problems have not been compared with other wheel rim designs. A theory of the finite element method for determining deformations and stresses has not been established. These will be done in the future.

The findings of this study offer a valuable design reference for automotive engineers seeking to improve fuel efficiency and ride quality through lightweight wheel components. Future work may involve experimental validation and adaptation of the optimized designs in real-world production settings.

Nomenclature

E	Young's modulus
σy	Yield strength
ρ	Density
ν	Poisson's ratio

Acknowledgement

The authors gratefully acknowledge the research support from Ho Chi Minh City University of Industry and Trade.

Compliance with ethics guidelines

The authors declare they have no conflict of interest or financial conflicts to disclose.

This article contains no studies with human or animal subjects performed by the authors.

References

Abhiman, B., Kumar, M. Y., & Reddy, M. V. R. (2021). Optimization of car rim using designing and analysis softwares. *International Journal of Research in Aeronautical and Mechanical Engineering, 9*(8), 1–6. https://doi.org/10.5281/ZENODO.52703

Alfarisi, S., Ariyansah, R., & Mugisidi, D. (2024). Finite Element Analysis of Aluminum Based R22 Car Wheel Design Modification. *Jurnal Asiimetrik: Jurnal Ilmiah Rekayasa dan Inovasi*, *6*(1–10). http://doi.org/10.35814/asiimetrik.v6i1.5077

DOI: 10.5614/j.eng.technol.sci.2026.58.4.9

Ashok, B., Naidu, M. K., & Rao, S. S. (2021). Design and weight optimization of aluminium alloy wheel rim for light weight four wheeled vehicle. *International Journal of Engineering Research & Technology, 10*(4), 484–490. https://doi.org/10.5281/zenodo.18620583

Barragán-Trinidad, M., Guadarrama-Pérez, O., Guillén-Garcés, R. A., Bustos-Terrones, V., Trevino-Quintanilla, L. G., & Moeller-Chávez, G. (2023). The Grey–Taguchi Method, a Statistical Tool to Optimize the Photo-Fenton Process: A Review. *Water*, *15*(15, 1–27). https://doi.org/10.3390/w15152685

Borchers, A., & Pieler, T. (2010). Programming pluripotent precursor cells derived from Xenopus embryos to generate specific tissues and organs. *Genes (Basel)*, *1*(3), 413–426. https://doi.org/10.3390/genes1030413

Ciardiello, F., & Genovese, A. (2023). A comparison between TOPSIS and SAW methods. *Annals of Operations Research*, *325*(2), 967-994. https://doi.org/10.1007/s10479-023-05339-w

artificial neural network method based on finite element analysis results

Solazzi, L., & Cima, M. (2024). Development of a FEM procedure for evaluating the pressure profile in the industrial wheel and fatigue strength analyses. *Journal of Applied Engineering Science*, *22*(2), 171–183. https://doi.org/10.5937/jaes0-48184

Dawson, J. W. (2025). Wheels integrity for UAH Moonbuggy ATHENA.

Fan, J., Lei, T., & Wu, M. (2024). MEREC-MABAC method based on cumulative prospect theory for picture fuzzy sets: Applications to wearable health technology devices. *Expert Systems with Applications*, *255*, 414–422. https://doi.org/10.1016/j.eswa.2024.124749

Gebrehiwet, L., Negussie, Y., & Tadesse, A. (2022). Business Opportunity of Wheel Rim Manufacturing in Ethiopia. International *Journal of Advances in Engineering and Management*, *4*(10), 1148–1159.

Gadwala, W. K., & Babu G, R. (2022). Modeling and analysis of car wheel rim for weight optimization to use additive manufacturing process. *Materials Today: Proceedings*, *62*, 336–345. https://doi.org/10.1016/j.matpr.2022.03.430

Hisam, M. W., Dar, A. A., Elrasheed, M. O., Khan, M. S., Gera, R., & Azad, I. (2024). The Versatility of the Taguchi Method: Optimizing Experiments Across Diverse Disciplines. *Journal of Statistical Theory and Applications*, *23*(4), 365–389. https://doi.org/10.1007/s44199-024-00093-9

Jakupi, K., Dukovski, V., & Abdullahu, F. (2024). Optimizing surface roughness of workpieces made of stainless steel 316L with DMLS technology: a Taguchi method approach. *Engineering Research Express*, *6*(2), 1–7. https://doi.org/10.1088/2631-8695/ad3db0

Jazaudhi'fi, A., Vitianingsih, A. V., Kristyawan, Y., Lidya Maukar, A., & Yasin, V. (2024). Recommendation System to Determine Achievement Students Using Naïve Bayes and Simple Additive Weighting (SAW) Methods. Digital Zone: *Jurnal Teknologi Informasi dan Komunikasi*, *15*(1), 67–79. https://doi.org/10.31849/digitalzone.v15i1.19746

Joglekar, A. A., Tripathi, V. K., Nagapurkar, S. J., & Netke, V. S. (2021). Design Optimization of Electric Vehicle Wheel using Composite Materials. *International Journal of Engineering Sciences*, *13*(4), 152–158. https://doi.org/10.36224/ijes.130403

Karim, H., & Ku, P. X. (2022). Effect of design and material on structural rigidity of automobile wheel - an optimisation approach. *Journal of Physics: Conference Series*, 2222, 1–13. https://doi.org/10.1088/1742-6596/2222/1/012007

Kepekci, H., Agca, M., & Komatina, M. (2025). Thermal and mechanical analysis of wheel rim in Formula 1 vehicles. *Thermal Science*, *29*(1 Part A), 325–335. https://doi.org/10.2298/tsci240721205k

Keshavarz-Ghorabaee, M. (2021). Assessment of distribution center locations using a multi-expert subjective-objective decision-making approach. *Sci Rep*, *11*(1), 19461. https://doi.org/10.1038/s41598-021-98698-y

Keshavarz-Ghorabaee, M., Amiri, M., Zavadskas, E. K., Turskis, Z., & Antucheviciene, J. (2021). Determination of Objective Weights Using a New Method Based on the Removal Effects of Criteria (MEREC). *Symmetry*, *13*(4), 525. https://doi.org/10.3390/sym13040525

Khatiwada, R., Giri, S., Khadka, R., & Mahat, C. (2025). Design, analysis and optimization of the wheel rim. *International Journal Of Research In Aeronautical And Mechanical Engineering*, *13*(4), 1-13.

Kruzel, R., Dembiczak, T., & Wachowicz, J. (2023). Optimization of Spark Plasma Sintering Technology by Taguchi Method in the Production of a Wide Range of Materials: Review. *Materials* (Basel), *16*(16), 1–18. https://doi.org/10.3390/ma16165539

Kumar, G. R. & Chandrashekhar, A. (2025). Design and analysis of a car wheel rim. *International Journal of Environmental Sciences*, *11*(17s), 1010–1016. https://doi.org/10.64252/62agff53

Loganathan, K., & Subramani, S. K. V. S. (2023). Design and optimization of aluminium alloy wheel rim in automobile industry. *Materials Today: Proceedings*. https://doi.org/10.1016/j.matpr.2023.01.207

Majumder, H., Gajghate, S. S., Sahu, A. R., Behera, A. K., Limbadri, C., & Ukey, K. (2023). Finite element analysis of wheel rim by additive manufacturing materials. *Materials Today: Proceedings*. *28*(2023), 341–349. https://doi.org/10.1016/j.matpr.2023.05.461

Montassir, S., Moustabchir, H., El Khalfi, A., Vlase, S., & Scutaru, M. L. (2024). Numerical Study of Crack Prediction and Growth in Automotive Wheel Rims. Materials (Basel), *17*(5), 1-14. https://doi.org/10.3390/ma17051020

Özdemir, Y. B., Karpuzcu, Y., Çam, S., & Günpınar, E. (2022). Wheel Rim Design Parametrization and Its Effect on Optimization. *Dokuz Eylul University Faculty of Engineering Journal of Science and Engineering*, *24*(72), 913–926. https://doi.org/https://doi.org/10.21205/deufmd.2022247220

Padmanabhan, S., Boopathi, B., Kumar, K. M., J. R, D., T, V. K., & S, B. (2023). Investigation of alloy materials on a sports bike wheel rim designs using finite element analysis. *Multidisciplinary Science Journal*, *6*(2), 1–9. https://doi.org/10.31893/multiscience.2024013

Padmanabhan, S., Kumar, T. V., Thiagarajan, S., Krishna, B. G., & Sudheer, K. (2023). Investigation of lightweight wheel design using alloy materials through structural analysis. *Materials Today: Proceedings*. 2023, 1–10. https://doi.org/10.1016/j.matpr.2023.01.013

Parihar, Y. P. S., & Chakraborty, A. (2022). Dynamic Design and Analysis of Car Wheel Rim Using FEA Method. *International Journal for Research in Applied Science and Engineering Technology*, *10*(5), 723–734. https://doi.org/10.22214/ijraset.2022.42319

Patil, G. H. & Chavan, H. A. (2023). Mathematical and Simulation Investigation of Automobile Wheel Rim Material. *International Journal of Progressive Research in Engineering Management and Science*, *3*(5), 878–888. https://doi.org/10.58257/IJPREMS31359

Roy, R. K. (2010). A primer on the Taguchi method. *Society of Manufacturing Engineers*, Second edition.

Santos, V. R. I., Scinocca, F., Almeida, L. G. N. d., & Santos, F. L. (2025). Virtual Development of Automotive Wheels: Modal, Vertical Impact and Fatigue Analysis and Simulation, using the finite element method. *Theoretical and Applied Engineering*, *9*(1), 1-20. https://doi.org/10.31422/taae.v9i1.63

Shanmugasundar, G., Sapkota, G., Čep, R., & Kalita, K. (2022). Application of MEREC in Multi-Criteria Selection of Optimal Spray-Painting Robot. Processes, 10(6), 1172. https://doi.org/10.3390/pr10061172

Sharma, A., Yadav, R., & Sharma, K. (2021). Optimization and investigation of automotive wheel rim for efficient performance of vehicle. *Materials Today: Proceedings*, *45*, 3601–3604. https://doi.org/10.1016/j.matpr.2020.12.1110

Shinde, T., Jomde, A., Shamkuwar, S., Sollapur, S., Naikwadi, V., & Patil, C. (2022). Fatigue analysis of alloy wheel using cornering fatigue test and its weight optimization. *Materials Today: Proceedings*, *62*, 1470–1474. https://doi.org/10.1016/j.matpr.2022.02.023

Somayaji, A., Marakala, N., Somayaji, S., & Hebbale, A. M. (2022). Studies on modal analysis of aluminium based carbon fibre reinforced optimized alloy wheel used in automotive sectors. *Materials Today: Proceedings*, *52*, 274–277. https://doi.org/10.1016/j.matpr.2021.08.099

Song, J., Lan, J., Zhu, L., Jiang, Z., Zhang, Z., Han, J., & Ma, C. (2024). Finite Element Simulation and Microstructural Analysis of Roll Forming for DP590 High-Strength Dual-Phase Steel Wheel Rims. *Materials* (Basel), *17*(15), 1–18. https://doi.org/10.3390/ma17153795

Tafazzoli, M., Hazrati, A., Shrestha, K., & Kisi, K. (2024). Enhancing Contractor Selection through Fuzzy TOPSIS and Fuzzy SAW Techniques. *Buildings*, 14(6), 1-24. https://doi.org/10.3390/buildings14061861

Taherdoost, H. (2023). Analysis of Simple Additive Weighting Method (SAW) as a MultiAttribute Decision-Making Technique: A Step-by-Step Guide. Journal of Management Science & Engineering Research, *6*(1), 21–24. https://doi.org/10.30564/jmser.v6i1.5400

Vinchu, A. T. & Chaudhari, D. S. (2021). Weight Optimization of Vehicle Rim with Fatigue Tests. *International Journal of Scientific Research & Engineering Trends*, *7*(3), 1680-1683.

Wacker, J. D., Laveuve, D., Contell Asins, C., & Büter, A. (2021). Design of a composite nose wheel for commercial aircraft. IOP Conf. Series: Materials Science and Engineering, *1024*, 1–8. https://doi.org/10.1088/1757-899X/1024/1/012018

Wang, Z., Wang, C., Yang, G., & Wu, F. (2022). Innovative Design of Automobile Wheel Rim Based on Honeycomb Features. *Journal of Engineering Management and Systems Engineering*, *1*(2), 67–75. https://doi.org/10.56578/jemse010204

Wijaya, V. I., Ariyansah, R., Agusman, D., & Heriyani, O. (2024). Analysis of vibration characteristics in 17-inch aluminum alloy wheel rims using finite element method. *Jurnal Asiimetrik: Jurnal Ilmiah Rekayasa dan Inovasi*, *6*(2), 283–294. https://doi.org/10.35814/asiimetrik.v6i2.6620

Zanchini, M., Longhi, D., Mantovani, S., Puglisi, F., & Giacalone, M. (2023). Fatigue and failure analysis of aluminium and composite automotive wheel rims: Experimental and numerical investigation. *Engineering Failure Analysis*, *146*, 1-20. https://doi.org/10.1016/j.engfailanal.2023.107064

DOI: 10.5614/j.eng.technol.sci.2026.58.4.9

Zhang, G., Tao, S., Zhou, Y., Ye, Z., Lu, J., Li, R., Li, S., Zhou, L., & Deng, T. (2025). Shape optimisation of rim structure of aluminium alloy car wheels based on 90 degrees impact test. *Sci Rep*, *15*(1), 24623. https://doi.org/10.1038/s41598-025-07802-z

Zhang, S., Lu, D., Li, R., Xu, L., Jiang, H., Cao, Y., & Xu, W. (2023). Fatigue life optimization and lightweight design of wheel based on entropy weight grey relation analysis and modified NSGA-II. *Advances in Mechanical Engineering*, *15*(8), 1–20. https://doi.org/10.1177/16878132231189119

Zhang, X., Liu, Y., & Wang, Z. (2025). Design and optimization of carbon fiber and magnesium alloy hybrid wheel rim. *Journal of Magnesium and Alloys*, *10*(4), 1024–1035.

Manuscript Received: 10 April 2025
1st Manuscript Revision Received: 18 September 2025
2nd Manuscript Revision Received: 1 December 2025
Accepted Manuscript: 26 May 2026